Solid-State Electronics 198 (2022) 108458

Contents lists available at ScienceDirect

Solid State Electronics

journal homepage: www.elsevier.com/locate/sse

Image-force barrier lowering in top- and side-contacted two-dimensional materials☆

Emeric Deylgat [a,b,c,*], Edward Chen [d], Massimo V. Fischetti [a], Bart Sorée [c,e,f], William G. Vandenberghe [a]

[a] Department of Materials Science and Engineering, The University of Texas at Dallas, 800 W. Campbell Road, Richardson, 75080-3021, TX, USA
[b] Department Physics, KU Leuven, Celestijnenlaan 200d, Leuven, 3001, Belgium
[c] Imec, Kapeldreef 75, Leuven, 3001, Belgium
[d] Corporate Research, Taiwan Semiconductor Manufacturing Company Ltd., 168 Park Ave. II Hsinchu Science Park, Hsinchu, 300-75, Taiwan
[e] Department of Electrical Engineering, KU Leuven, Kasteelpark Arenberg 10, Leuven, 3001, Belgium
[f] Department of Physics, Universiteit Antwerpen, Groenenborgerlaan 171, Antwerp, 2020, Belgium

ARTICLE INFO

Keywords:
Two-dimensional materials
Side-contact
Top-contact
Image force barrier lowering
WKB-approximation

ABSTRACT

We compare the image-force barrier lowering (IFBL) and calculate the resulting contact resistance for four different metal–dielectric-two-dimensional (2D) material configurations. We analyze edge contacts in three different geometries (a homogeneous dielectric throughout, including the 2D layer; a homogeneous dielectric surrounding the 2D layer, both ungated and back gated) and also a top-contact assuming a homogeneous dielectric. The image potential energy of each configuration is determined and added to the Schottky energy barrier which is calculated assuming a textbook Schottky potential. For each configuration, the contact resistivity is calculated using the WKB approximation and the effective mass approximation using either SiO_2 or HfO_2 as the surrounding dielectric. We obtain the lowest contact resistance of 1 kΩ µm by n-type doping an edge contacted transition metal-dichalcogenide (TMD) monolayer, sandwiched between SiO_2 dielectric, with $\sim 10^{12}$ cm^{-2} donor atoms. When this optimal configuration is used, the contact resistance is lowered by a factor of 50 compared to the situation when the IFBL is not considered.

1. Introduction

Making low-resistance contacts to two-dimensional (2D) materials is challenging and the theory behind contacts is not well-developed [1–3]. The metal/transition-metal dichalcogenide (TMD) interface often introduces a contact resistance of >1 kΩ µm [4] due to large Schottky barriers at the interface. Most studies of edge or top contacts ignore the impact of image-force barrier lowering (IFBL) on the Schottky barrier [5] which is crucial to accurately estimate the contact resistance in different situations. Recently, we calculated the contact resistance in side contacts, using a semiclassical model but accounting for IFBL [6], and showed that using a low-κ dielectric around the 2D material drastically improves contact resistance.

In this work, we analyze the impact of the IFBL in four different metal–dielectric-2D material configurations as illustrated in Fig. 1(a)–(d). Fig. 1(a) shows the "hom" configuration, consisting of an edge contact (EC) to the TMD assuming the dielectric response of the 2D material is the same as that of the dielectric. In (b), we account for the dielectric response of the MoS_2 monolayer with $t_{2D} = 0.65$ nm [7] (the "het" configuration). In (c), we introduce a metal back-gate at a distance of $L_{EOT} = 1$ nm (the "gated" configuration). Finally, we investigate a top contact to the TMD assuming a homogeneous dielectric environment as shown in (d), where $t_{VdW} = 0.2$ nm [3] (the "top" configuration). We determine the IFBL in each of the configurations and calculate the resulting contact resistance as a function of n-type doping of the 2D channel material with surrounding dielectrics of either SiO_2 or HfO_2.

2. Methodology

In the "hom" configuration, we use the textbook IFBL expression (Eq. (1)) obtained using the well-known method of images [8]

$$U_{\text{image}}^{\text{hom}}(x) = -\frac{e^2}{8\pi\epsilon}\frac{1}{2x}. \quad (1)$$

☆ The review of this paper was arranged by Francisco Gamiz.

* Corresponding author at: Department of Materials Science and Engineering, The University of Texas at Dallas, 800 W. Campbell Road, Richardson, 75080-3021, TX, USA.
E-mail address: emeric.deylgat@utdallas.edu (E. Deylgat).

https://doi.org/10.1016/j.sse.2022.108458

Available online 22 September 2022

$$\hat{V}^{\text{gated}}(Q) = \frac{\left[\epsilon_{2\text{D}} \cosh\left(\frac{1}{2}\beta t_{2\text{D}} Q\right) + \epsilon \sinh\left(\frac{1}{2}\beta t_{2\text{D}} Q\right)\right]^2 + \left[\epsilon^2 \sinh^2\left(\frac{1}{2}\beta t_{2\text{D}} Q\right) - \epsilon_{2\text{D}}^2 \cosh^2\left(\frac{1}{2}\beta t_{2\text{D}} Q\right)\right] e^{-2\beta L Q}}{2Q\left\{\epsilon_{2\text{D}}^2 \epsilon \cosh(\beta t_{2\text{D}} Q) + \epsilon_{2\text{D}} \sinh(\beta t_{2\text{D}} Q)\left[\epsilon^2\left(1 + e^{-2\beta L Q}\right) + \epsilon_{2\text{D}}^2\left(1 - e^{-2\beta L Q}\right)\right]\right\}}. \tag{3}$$

Box I.

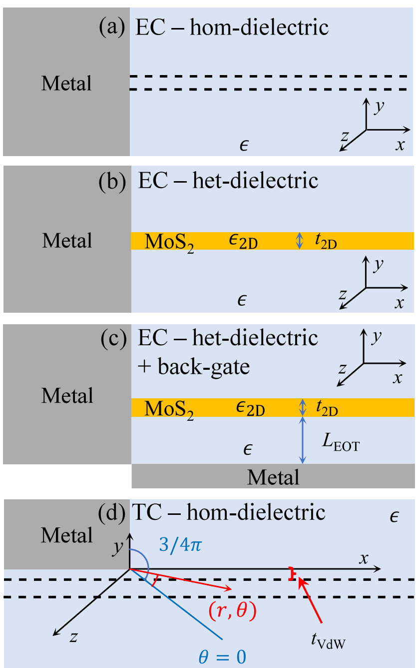

Fig. 1. (a) Edge contact (EC) with homogeneous dielectric ("hom"); (b) EC with heterogeneous dielectric ("het"); (c) EC with heterogeneous dielectric and metal back-gate ("gated"); (d) Top contact (TC) with a homogeneous dielectric ("top").

Here, $\epsilon = \epsilon_0 \epsilon_r$, where ϵ_r is the relative dielectric constant of the surrounding dielectric, which is either $\epsilon_r = \epsilon_{\text{SiO}_2} = 3.9$ or $\epsilon_r = \epsilon_{\text{HfO}_2} = 25$. In Ref. [9], we obtained the IFBL for "het" and "gated" ("h/g") configurations using the method of images yielding a Hankel transform

$$U_{\text{image}}^{\text{h/g}}(x) = -\frac{e^2}{4\pi}\int_0^{\infty} \hat{V}^{\text{h/g}}(Q) J_0(2xQ) Q dQ. \tag{2}$$

Here, $\hat{V}^{\text{h/g}}(Q)$ is the Hankel transform of the potential due to a point charge in the "het" or "gated" configurations and J_0 is the zeroth order Bessel function of the first kind. $\hat{V}^{\text{h/g}}(Q)$ can be derived with laborious algebra (omitted here) and, for the "gated" configuration takes the form (see Box I) where, $\epsilon_{2\text{D}} = \sqrt{\epsilon_{\parallel}\epsilon_{\perp}}$ and $\beta = \sqrt{\epsilon_{\parallel}/\epsilon_{\perp}}$. The limit $L \to \infty$ gives $\hat{V}^{\text{het}}(Q)$ for the "het" geometry. For the top contact, we derive the IFBL using the Kontorovich–Lebedev transform [10] which yields

$$\tilde{U}_{\text{image}}^{\text{top}}(r,\theta) = -\frac{e^2}{8\pi\epsilon}\frac{1}{r}\left[\frac{1}{2} - \frac{2}{3\sqrt{3}} + \int_0^{\infty} \frac{\cosh(2\alpha\theta)}{\sinh(\alpha\frac{3\pi}{2})} \tanh(\alpha\pi) d\alpha\right]. \tag{4}$$

Using transformations $r = \sqrt{x^2 + y_0^2}$ and $\theta = \operatorname{atan}(x/y_0)$, we define the potential $U_{\text{image}}^{\text{top}}(x)$ along the 2D layer at $y_0 = -t_{\text{VdW}} - t_{2\text{D}}/2$.

To estimate the impact of the IFBL on contact resistivity, we consider a conventional Schottky barrier potential [11]

$$U_{\text{S}}(x) = \frac{eN_{\text{D}}}{2\epsilon}(x - x_{\text{dep}})^2, \text{ and } x_{\text{dep}} = \sqrt{\frac{2\epsilon\phi_{\text{S}}}{eN_{\text{D}}}}. \tag{5}$$

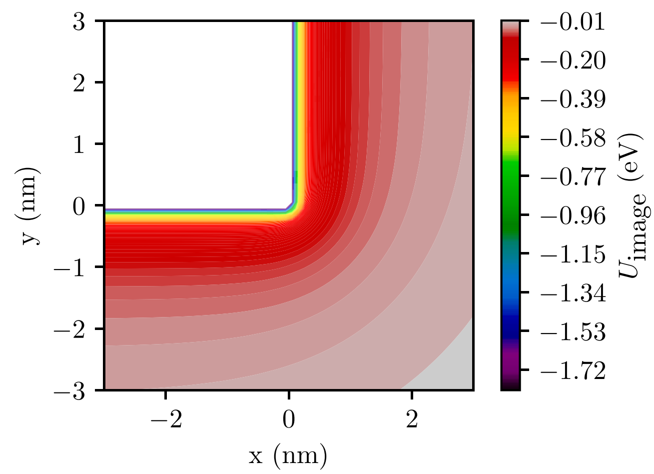

Fig. 2. Image potential energy for a top contact configuration (d), where SiO_2 is chosen as the surrounding dielectric.

Here, N_{D} is the n-type doping concentration and ϕ_{S} is the Schottky-barrier height. The total potential-energy barrier is given by $U(x) = U_{\text{S}}(x) + U_{\text{image}}(x)$. We follow Ref. [12,13] to compute the contact resistivity ρ_c

$$\frac{1}{\rho_c} = \frac{2e^2}{h}\int_{-\infty}^{+\infty} dE \left|\frac{df(E)}{dE}\right| \int_{-\infty}^{+\infty} \frac{dk_y}{2\pi} T(k_y, E) \tag{6}$$

where $\left|\frac{df(E)}{dE}\right|$ is the first derivative of Fermi–Dirac equation, $U(x)$ is the potential energy, E is the total energy, k_y is the y-component of the k-vector and $T(k_y, E)$ is given by the WKB approximation

$$T(k_y, E) = \exp\left[-2\int_0^{x_{\text{dep}}} \kappa(x) dx\right]. \tag{7}$$

Assuming that the effective mass m^* of MoS_2 is $m^* = 0.5 m_e$, we compute $\kappa(x)$ as

$$\kappa(x) = \sqrt{\frac{2m^*}{\hbar^2}\left(E - \left(U(x) + \frac{\hbar^2 k_y^2}{2m^*}\right)\right)}. \tag{8}$$

3. Results

In Fig. 2, we show the IFBL due to an electron in the vicinity of a metal wedge as presented in Eq. (4). We observe that the electron experiences an attractive force towards the metal since the image potential energy $\tilde{U}_{\text{image}}^{\text{top}}(r,\theta)$ decreases coming closer to the wedge.

Fig. 3 shows the image potential energy as a function of distance x from the interface in the center of the TMD. The "hom" configuration expresses the overall strongest IFBL compared to all other configurations. The "het" configuration shows reduced IFBL for very small x, while the "gated" configuration has much lower IFBL for large x. For the "top" configuration, we take a slice of Fig. 2 at $y = -0.525$ nm where the middle of the TMD would be. As a result of the slice not reaching a metal plate, configuration (d) has the lowest IFBL at small x compared to all other configurations.

Fig. 4 plots a "position-dependent" dielectric constant which is defined to yield the correct image-force potential in the middle of

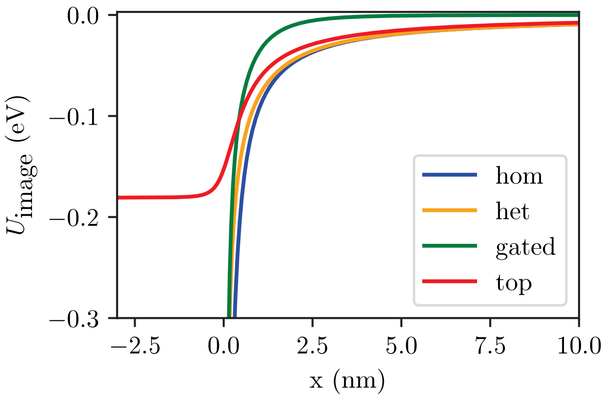

Fig. 3. Image potential energy profiles for the various contact configurations accounting for a surrounding dielectric of SiO_2.

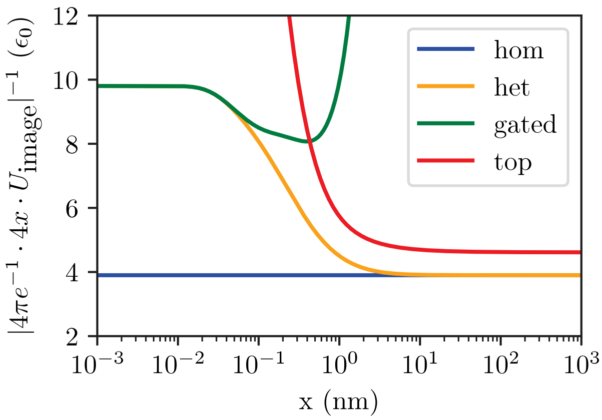

Fig. 4. The "position-dependent" dielectric constant $\epsilon(x)$ vs. x for every contact configuration. It compares the behavior of U_{image} in each configuration to the expected textbook behavior as defined in Eq. (1).

the layer in all configurations when using Eq. (1). This quantity can be defined as $\epsilon(x) = \left|4\pi e^{-1} \cdot 4x \cdot U_{\mathrm{image}}(x)\right|^{-1}$. For the "hom" configuration, the "position-dependent" dielectric constant remains close to the dielectric constant of the environment which is in this case $\epsilon_{SiO_2} = 3.9\epsilon_0$. For the "het" and "gated" configurations, the dielectric constant approaches $\epsilon_{2D} = 9.8\epsilon_0$ for $x < t_{2D}$. The dielectric constant of the 2D material controls the behavior of the image potential close to the metal. As a result, the potential goes as $1/(\epsilon_{2D}x)$. For $x > t_{2D}$, the "position-dependent" dielectric constant in the "het" configuration tends to $\epsilon_{SiO_2} = 3.9\epsilon_0$, while in the "gated" configuration it diverges to infinity as the image potential is influenced by the back-gate metal. In the "top" configuration, the dielectric constant diverges to infinity for $x \ll 0$ which is due to the flat potential profile of the image potential under the metal. At $x \gg 0$, the potential settles at a higher dielectric constant of $\epsilon = 4.62\epsilon_0 > \epsilon_{SiO_2}$ compared to the surrounding dielectric, implying that U_{image} is less steep than in the "hom" and "het" configurations.

Fig. 5 illustrates the tunnel barriers with a Schottky-barrier height $\phi_S = 0.3$ eV, $N_D = 10^{10}$ cm^{-2} and a surrounding dielectric of SiO_2 ($\epsilon_{SiO_2} = 3.9\epsilon_0$) for all configurations. At all distances from the metal plates, the barrier is most reduced in the case of the "hom" configuration, closely followed by the "het" configuration. When close to the metal, the Schottky barrier is lower for the "gated" configuration compared to the "top" configuration, while the reverse is true at a large distance from the metal plate.

In Fig. 6 we show the contact resistance (Eq. (6)) as a function of doping concentration for all contact configurations with surrounding

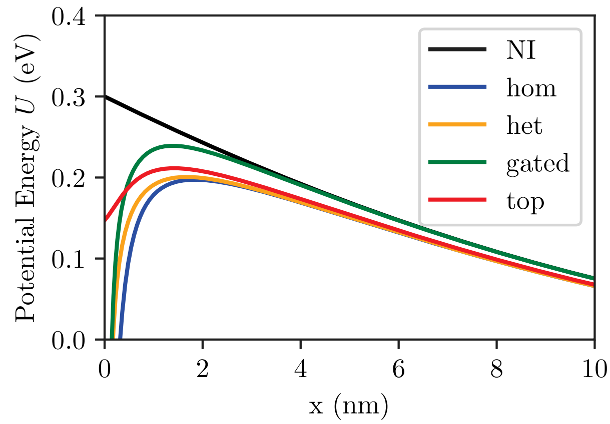

Fig. 5. Potential energy $U(x) = U_S + U_{\mathrm{image}}$. The Schottky barrier is plotted in case of no IFBL contributions (NI) and in case of all contact configurations. The surrounding dielectric used for this plot is SiO_2.

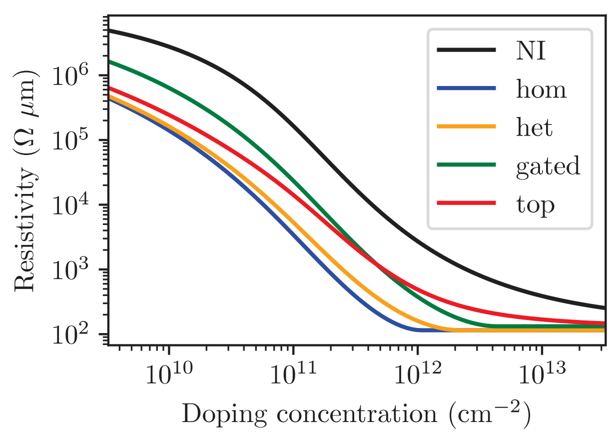

Fig. 6. Contact resistivity vs. doping concentration for a SiO_2 surrounding dielectric: NI - No IFBL, (a)–(d) with IFBL in all contact configurations.

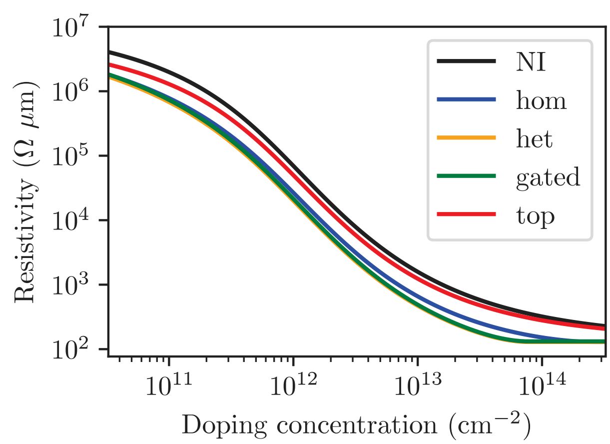

Fig. 7. Contact resistivity vs. doping concentration for a HfO_2 surrounding dielectric: NI - No IFBL, (a)–(d) with IFBL in all contact configurations.

SiO_2 ($\epsilon = 3.9\epsilon_0$) dielectric. A contact resistivity of 115 $\Omega\,\mu$m is obtained at a doping of $\sim 10^{12}$ cm^{-2} using side contact configurations.

In Fig. 7, we show the contact resistance in each contact configuration with HfO_2 as surrounding dielectric ($\epsilon = 25\epsilon_0$). We observe that a contact resistance of 130 $\Omega\,\mu$m is achieved at a doping of 10^{14} cm^{-2} using side-contact configurations. Compared to the contacts surrounded by SiO_2, we need to increase the doping concentration in

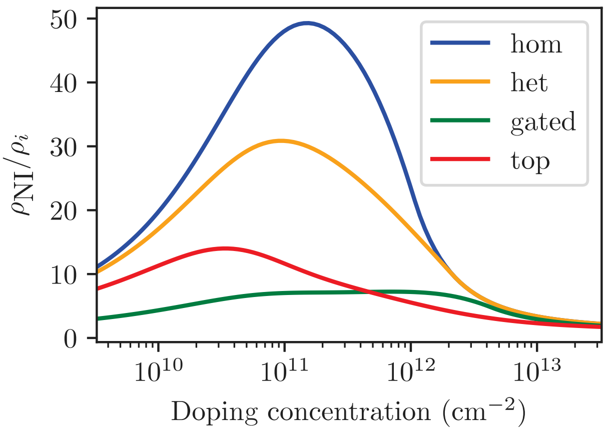

Fig. 8. Ratio of Schottky resistivity w/o IFBL (ρ_{NI}) and the resistivity of the various contact configurations (ρ_i; i =) (a)–(d) for a SiO_2 surrounding dielectric.

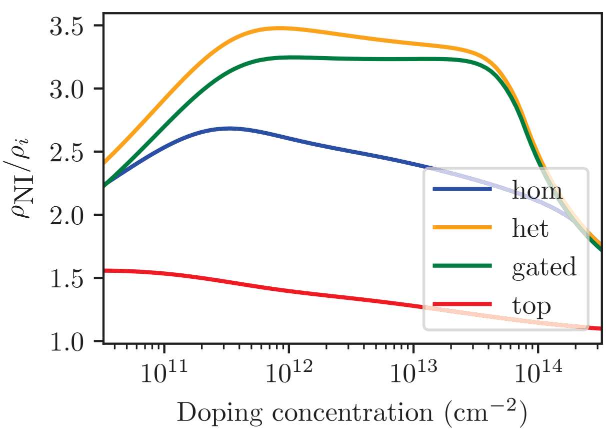

Fig. 9. Ratio of Schottky resistivity w/o IFBL (ρ_{NI}) and the resistivity of the various contact configurations (ρ_i; i =) (a)–(d) for a HfO_2 surrounding dielectric.

the 2D material by two orders of magnitude to realize a similar contact resistance when using a higher-κ dielectric.

Fig. 8 plots the ratios of the resistivity for the Schottky barrier with IFBL and without IFBL contribution in a surrounding dielectric of SiO_2, while Fig. 9 shows the ratios with a surrounding dielectric of HfO_2. When using SiO_2, the contact resistance experiences the largest improvement in the "hom" configuration of about 50, while using the more realistic "het" configuration, we still obtain a considerably large improvement of about 30. The configuration with a back-gate and the top contact configuration yield smaller improvements of only ~15 and ~10, respectively. Substituting the surrounding dielectric for HfO_2, the more realistic "het" and "gated" edge contact configurations show the biggest improvements of ~3.6 and ~3.4, respectively. The "hom" configuration shows an improvement in contact resistance of ~2.7, while the top contact only shows an improvement ~1.5.

4. Conclusion

In conclusion, we find that the IFBL in the "het" side contact combined with SiO_2 as dielectric improves the contact resistances up to three times compared to the top contact. Using low-κ surrounding dielectric materials such as SiO_2 greatly reduces contact resistance (up to ten times) compared high-κ materials such as HfO_2. Back-gating yields higher contact resistances compared to contacts without back-gate. However, at high doping, the resistance of a back-gated contact can be lower than that of a top contact. The resistances of the order $\sim 100\ \Omega\,\mu\mathrm{m}$ are optimistic, but the model used for the depletion of the TMD has limitations. In future work, we will use more accurate models to determine the depletion leading to better estimates of the contact resistivity.

Declaration of competing interest

The authors declare that they have no known competing financial interests or personal relationships that could have appeared to influence the work reported in this paper.

Data availability

Data will be made available on request.

Acknowledgments

This work has been supported by the Taiwan Semiconductor Manufacturing Company, Ltd. and the NEWLIMITS/nCORE program of the Semiconductor Research Corporation (SRC), USA.

References

[1] English CD, Shine G, Dorgan VE, Saraswat KC, Pop E. Improved contacts to mos2 transistors by ultra-high vacuum metal deposition. Nano Lett 2016;16:3824–30, PMID: 27232636.
[2] Mleczko MJ, Yu AC, Smyth CM, Chen V, Shin YC, Chatterjee S, et al. Contact engineering high-performance n-type mote2 transistors. Nano Lett 2019;19:6352–62, PMID: 31314531.
[3] Kang J, Liu W, Sarkar D, Jena D, Banerjee K. Computational study of metal contacts to monolayer transition-metal dichalcogenide semiconductors. Phys Rev X 2014;4:031005.
[4] Allain A, Kang J, Banerjee K, Kis A. Electrical contacts to two-dimensional semiconductors. Nature Mater 2015;14:1195–205.
[5] Szabó A, Jain A, Parzefall M, Novotny L, Luisier M. Electron transport through metal/mos2 interfaces: Edge- or area-dependent process? Nano Lett 2019;19:3641–7, PMID: 31079463.
[6] Brahma M, Van de Put ML, Chen E, Fischetti MV, Vandenberghe WG. Modeling contact resistivity in monolayer molybdenum disulfide edge contacts. In: 2021 international conference on simulation of semiconductor processes and devices. 2021, p. 175–9. http://dx.doi.org/10.1109/SISPAD54002.2021.9592589.
[7] Yoon Y, Ganapathi K, Salahuddin S. How good can monolayer mos2 transistors be? Nano Lett 2011;11:3768–73, PMID: 21790188.
[8] Griffiths DJ. Introduction to electrodynamics. 4th ed.. Pearson, Boston, MA; 2013, Re-published by Cambridge University Press in 2017.
[9] Brahma M, Van de Put ML, Chen E, Fischetti MV, Vandenberghe WG. Contacts to two-dimensional materials: Image forces, dielectric environment, and back-gate. In: 2022 international symposium on VLSI technology, systems and applications (VLSI-TSA). 2022, p. 1–2. http://dx.doi.org/10.1109/VLSI-TSA54299.2022.9770997.
[10] Kontorovich M, Lebedev N. On the one method of solution for some problems in diffraction theory and related problems. Zh Eksp Teor Fiz 1938;8:1192–206.
[11] Sze SM. Semiconductor devices: physics and technology. John wiley & sons; 2008.
[12] Vandenberghe WG, Verhulst AS, Kao K-H, Meyer KD, Soré B, Magnus W, et al. A model determining optimal doping concentration and material's band gap of tunnel field-effect transistors. Appl Phys Lett 2012;100:193509.
[13] Duke C. Tunneling in solids, solid state physics. Academic Press; 1969.